LBL-41608

Ferrofluid Flow for TOUGH2

Curtis M. Oldenburg and George J. Moridis

Earth Sciences Division
Berkeley Lab
Berkeley, CA, 94720

ABSTRACT

Ferrofluids are suspensions of magnetite particles with average diameter of order 10 nm stabilized by surfactants in carrier liquids. The potential applicability of ferrofluids to subsurface environmental engineering has recently been recognized. In one potential environmental engineering application, externally applied magnetic fields are used to control and direct the flow of ferrofluids underground. In order to facilitate the design and experimentation of porous media ferrofluid applications, we have developed a TOUGH2 module called EOS7M for simulating the flow and transport of ferrofluid. In the presence of an external magnetic field, the ferromagnetic colloidal particles suspended in the carrier liquid of a ferrofluid become magnetized and produce attractive forces on each particle that produce a body force on the liquid. The steps involved in calculating ferrofluid flow are (1) calculation of the external magnetic field and its gradient, (2) calculation of the ferrofluid magnetization, (3) calculation of the magnetic force on the fluid, (4) addition of the magnetic force to the pressure gradient and gravitational body force terms, and (5) calculation of the resulting liquid phase fluxes. These methods along with simple density and viscosity relations for the aqueous phase as a function of the mass fraction of ferrofluid have been implemented in a module called EOS7M. Example calculations that model laboratory experiments have been carried out to validate the methods.

INTRODUCTION

Ferrofluids are suspensions of single domain magnetite particles with average diameters of approximately 10 nm stabilized by surfactants in carrier liquids (Rosenzweig, 1985; Berkowsky *et al.*, 1993). Ferrofluids have found applications in a variety of engineered devices and systems for, among other things, lubrication and sealing of bearings (Raj and Moskowitz, 1990). Recently, their potential utility in subsurface environmental engineering has been recognized (Moridis *et al.*, 1998). In one potential environmental engineering application, externally applied magnetic fields are used to control and direct the flow of ferrofluids underground. We call the driving force on the ferrofluid generated by the application of an external magnetic field magnetopressure. Carefully applied magnetopressure could be useful for creating and testing subsurface barriers, grouting rock for strength, and directing injected chemical agents and microbes toward particular contaminated zones.

In order to facilitate the design and experimentation of porous media ferrofluid applications, as well as to carry out numerical experiments of ferrofluid flow phenomena, we have developed simulation capability for ferrofluids. This simulation capability is being built upon the TOUGH2 framework (Pruess, 1987; 1991a) as an equation of state module called EOS7M (Oldenburg *et al.*, 1998a). The purpose of this paper is to summarize the equations and methods used to simulate the flow of ferrofluids in porous media and to present example simulations from EOS7M.

MATHEMATICAL DEVELOPMENT

Magnetic Force

In the presence of an external magnetic field, the single-domain colloidal magnetite particles suspended in the carrier liquid of a ferrofluid become magnetized (Fig. 1). The magnetization or polarization of the fluid interacts with the external magnetic field to produce attractive forces on each particle. By virtue of the suspension of ferrofluid particles in the liquid, the attractive magnetic force manifests itself as a body force on the liquid, analogous to the body force on a liquid due to gravity. The attractive force on ferrofluid per unit volume is given by

$$\boldsymbol{F} = \mu_o \, M \nabla H \qquad (1)$$

where μ_o is the magnetic permeability of free space (Tesla m/Ampere-turn), M is the magnetization (Ampere-turn/m), and H is the magnetic field

strength of the external magnetic field (Ampere-turn/m). The units of Eq. 1 are thus

$$\frac{N}{m^3} [=] \frac{Tm}{A} \frac{A}{m} \frac{A}{m^2} [=] \frac{TAm}{m^3} \quad (2).$$

Thus the calculation of the magnetopressure involves calculating H, ΔH, and M, along with the ferrofluid mass fraction at each gridblock. The remainder of this section outlines the methods for calculating these quantities.

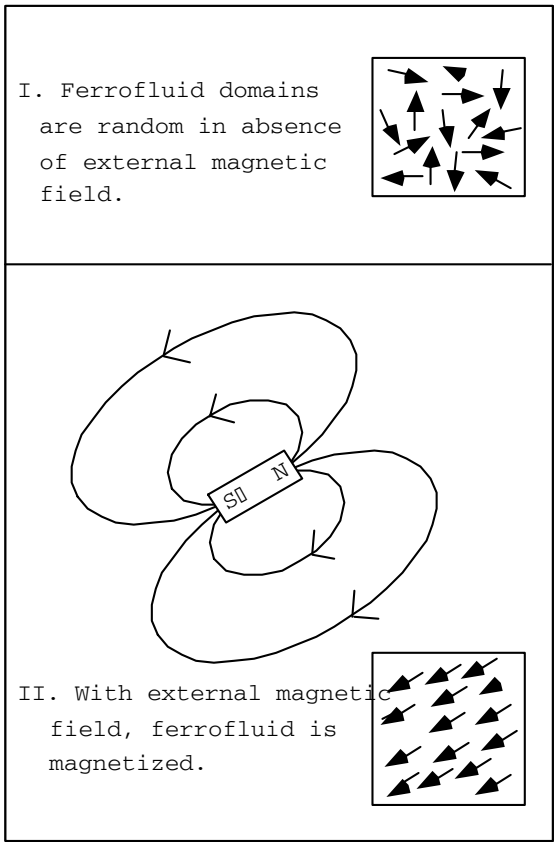

Fig. 1. Polarization of ferrofluid particles.

Magnetic Field Strength

The calculation of magnetic field strength is complicated for general systems with variable magnetic permeability. However, if the medium is free of ferromagnetic minerals and a permanent magnet is the source of the magnetic field, we can use some simple equations to calculate the components of H directly. These direct equations were presented with an error in McCaig (1977) and corrected in McCaig and Clegg (1987). In the direct equations, the poles of the magnet are a distance L apart, and the field at any location is the difference between the fields due to each pole. The full equations are too lengthy to include here, but are presented in full in Oldenburg *et al.* (1998b). Along the Z-axis assumed perpendicular to the face of either the North or South pole of a rectangular magnet (Fig. 2), the equation for the Z component of H simplifies to

$$H_z = \frac{B_r}{\pi \mu_0} \left[\tan^{-1}\left(\frac{ab}{z\left(a^2+b^2+z^2\right)^{1/2}} \right) - \tan^{-1}\left(\frac{ab}{(z+L)\left(a^2+b^2+(z+L)^2\right)^{1/2}} \right) \right] \quad (3)$$

where B_r is the residual flux density of the permanent magnet. The magnetic field strength (H) needs only to be calculated once at the beginning of the simulation for all gridblocks in the domain. The gradient of H is calculated by simple differencing at each gridblock interface.

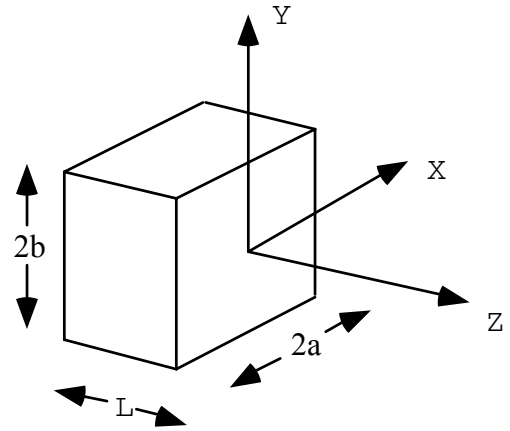

Fig. 2. Local coordinate system for the magnetic field produced by a permanent magnet.

Magnetization

As the strength of an external magnetic field is increased from zero A/m, pure ferrofluid will become magnetized to a degree controlled by the strength of the external field and the properties of the ferrofluid. The relationship between the magnetic induction (B), and magnetic field strength (H), and magnetization (M) is known as the B-H curve, where

$$\mathbf{B} = \mu_o(\mathbf{H} + \mathbf{M}) \quad (4).$$

Eq. 4 has been written in terms of the vectors **B, H**, and **M**, but can also be written as a scalar equation where B, H, and M are scalars representing the corresponding vector magnitudes. As the external magnetic field is increased, the ferrofluid reaches a maximum magnetization, or saturation magnetization. Thus the magnetization is a function (f) of H whose parameters depend on the particular

type and size of the ferromagnetic material in the fluid:

$$M = f(H) \qquad (5)$$

An example magnetization curve and an arctangent function model fit for the ferrofluid EMG 805 (Ferrofluidics, NH) is shown in Fig. 3.

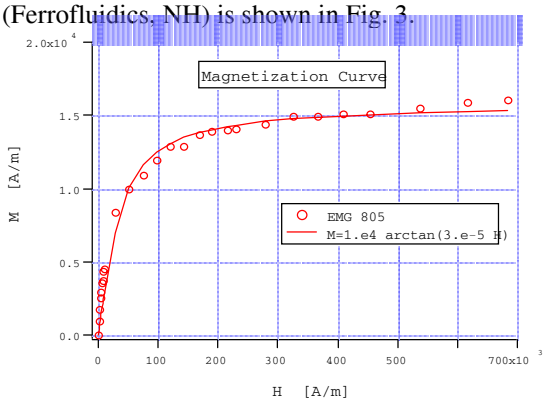

Fig. 3. Magnetization data and arctangent curves used to model ferrofluid magnetization. The arctangen functions are of the form $M = a1$ arctan $(b1*H)$.

Mixing Model

The ferrofluid in EOS7M is assumed to be miscible with water, giving rise to a single aqueous phase with components (1) water and (2) ferrofluid pseudo component. Following the work of Reeves *et al.* (1986) and Herbert *et al.* (1988) on brine-water mixtures, we use the simple mixing models as in EOS7 (Pruess, 1991b) where density and viscosity are given by

$$\frac{1}{\rho} = \frac{1 - X_{ff}}{\rho_w} + \frac{X_{ff}}{\rho_{ff}} \qquad (6)$$

$$f(X_{ff}) = 1 + \mu(1) X_{ff} + \mu(2) X_{ff}^2 + \mu(3) X_{ff}^3 \quad (7)$$

where the density of the two components are given by ρ_w and ρ_{ff}, and the last two terms in Eq. 7 have been neglected due to lack of data. The magnetization (M) of the water-ferrofluid mixture is assumed to be directly proportional to the ferrofluid mass fraction:

$$M = M_{(X_{ff}=1)} X_{ff} \quad (8).$$

Transport parameters controlling processes such as dispersivity, diffusivity, adsorption, and straining are poorly known and are not currently included in EOS7M. Similarly, the non-isothermal behavior of magnetic materials is complicated and we currently restrict EOS7M to isothermal conditions at 20˚C.

Solution Methodology

After the magnetic field strength and its gradient are calculated by the use of the direct equations, the magnetic body force must be included in a set of flow equations that includes conservation of ferrofluid component. We have used the TOUGH2 (Pruess, 1987; Pruess, 1991a) framework and developed a module called EOS7M (Oldenburg *et al.*, 1998a) for ferrofluid flow and transport for TOUGH2. The integral conservation equations solved by the integral finite difference method in TOUGH2 consist of balances between mass accumulation and flux and source terms over all grid blocks V_n into which the flow domain V has been partitioned:

$$\frac{d}{dt}\int_{V_n} M^{(\kappa)} dV = \int_{\Gamma_n} F^{(\kappa)} \cdot n \, d\Gamma + \int_{V_n} q^{(\kappa)} dV \qquad (9)$$

In Eq. 9, the index n = 1, ..., N corresponds to the grid blocks with volume V_n and surface area Γ_n. The index κ = 1, ..., NK+1 corresponds to the NK fluid components and heat. The mass accumulation term (M) in Eq. 9 is given by

$$M^{(\kappa)} = \phi \sum_{\beta=1}^{NPH} S_\beta \rho_\beta X_\beta^{(\kappa)} \qquad (10)$$

The flux term can be written

$$\boldsymbol{F}^{(\kappa)} = \sum_{\beta=1}^{NPH} X^{(\kappa)} \boldsymbol{F}_\beta \qquad (11)$$

where hydrodynamic dispersion and molecular diffusion have been neglected. Eq. 11 accounts for the flux of component κ arising from Darcy flux of the phases containing κ. With the inclusion of magnetic forces along with the usual pressure gradient and gravitational body forces, the phase flux term for a single phase (β subscript dropped) can be written

$$\boldsymbol{F} = \rho \mathbf{u} = -\frac{k}{\mu} \rho (\nabla P - \rho \mathbf{g} - \mu_o M \nabla H) \qquad (12).$$

As shown in Eqs. 6, 7, 8, and 12, the forces on ferrofluid depend on the ferrofluid mass fraction. Therefore, flow of ferrofluid is strongly coupled to ferrofluid transport. This type of strongly coupled flow problem is analogous to variable density flow problems with large density changes and requires strongly coupled solution techniques (Oldenburg and Pruess, 1995) such as those used in TOUGH2.

In EOS7M, we calculate the external magnetic field once at the beginning of each simulation. The coupling between ferrofluid flow and the external

magnetic field occurs through the *M* and □*H* terms. Magnetization is modeled using the arctangent function (Fig. 3) and the assumption that magnetization is a linear function of ferrofluid mass fraction. Then the magnetic force at the interface between each gridblock is calculated and added to the pressure gradient and gravitational body force terms. A diagram showing the calculation procedure is presented in Fig. 4.

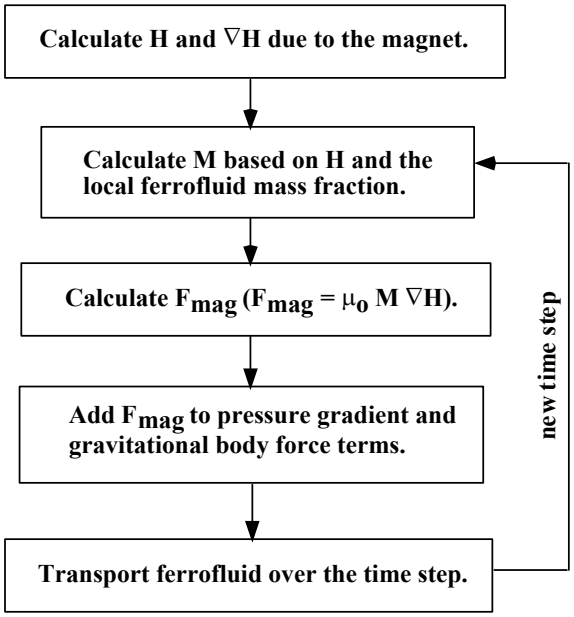

Fig. 4. Schematic of ferrofluid flow calculation implemented in EOS7M.

EXAMPLE SIMULATIONS

We present next two example simulations of (1) the magnetopressure generated, and (2) the two-dimensional flow of ferrofluid in response to an external magnetic field. The first simulation models a laboratory experiment in which five 2 inch x 2 inch x 1 inch NdFeB permanent magnets are moved toward a small horizontal tube that is open to atmospheric pressure on one end and connected to a pressure transducer (DP 15-26, Validyne Engineering Corp.) on the other end (Borglin *et al.*, 1998). The tube is aligned with the magnetic poles. The pressures are measured and recorded resulting in a plot of ferrofluid pressure *versus* distance where the pressure is due to the force on the ferrofluid as given by Eq. 1. Shown in Fig. 5 is the comparison between measured pressures and pressures calculated using EOS7M. The agreement is good. In the experiment it was observed that the ferrofluid develops spikes near the magnet at the interface with the oil in the tube connected to the pressure transducer. These spikes are analogous to the chains of dry magnetite particles that follow magnetic lines of flux in a strong magnetic field. These effects are not modeled in EOS7M and may have contributed to the smaller experimental pressures compared to the simulated pressures at high field strength near the magnet. We note that because the polarization of ferrofluid is caused by the external magnetic field, it does not matter whether the magnet is aligned with the north pole or the south pole closest to the pressure transducer end of the tube; the force on the ferrofluid is always attractive, and the pressure always increases at the end closer to a magnet regardless of its polarization.

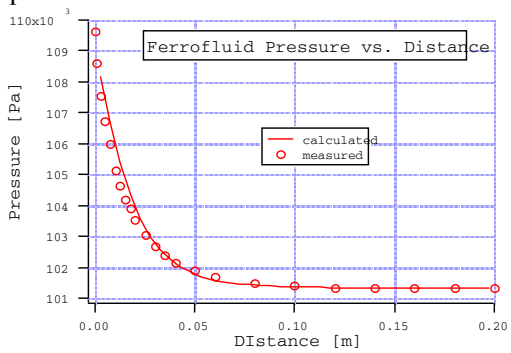

Fig. 5. Measured and calculated ferrofluid pressures versus distance from a permanent magnet.

In the second example simulation, we model the two-dimensional flow of ferrofluid in a narrow gap between two glass plates (a Hele-Shaw cell). This experiment was also carried out in the lab. We present first in Fig. 6 the external magnetic field calculated using EOS7M due to the magnet at the right-hand side of the domain. Properties of the system are presented in Table 1.

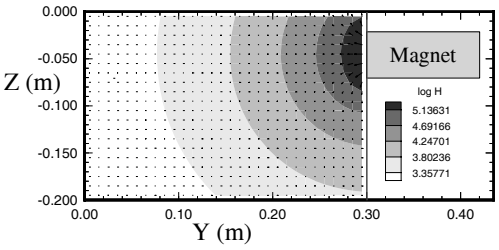

Fig. 6. Magnetic field (*H*) in units of log A/m around magnet in Hele-Shaw cell experiment.

Shown in Fig. 7 is the two-dimensional ferrofluid mass fraction field along with velocity vectors at three different times. The initial condition (upper

left-hand frame of Fig. 7) has a small pool of pure ferrofluid in the lower left-hand corner and a magnet at the upper right-hand corner. The gap is filled with colloidal silica, a dense liquid chosen to minimize the density difference between ferrofluid and the background fluid (see Table 4). As such, the viscosity of the pure water aqueous phase in EOS7M was set specially for this simulation to 4.5×10^{-3} Pa s to model the laboratory experiment which used colloidal silica in the gap, while the viscosity of pure

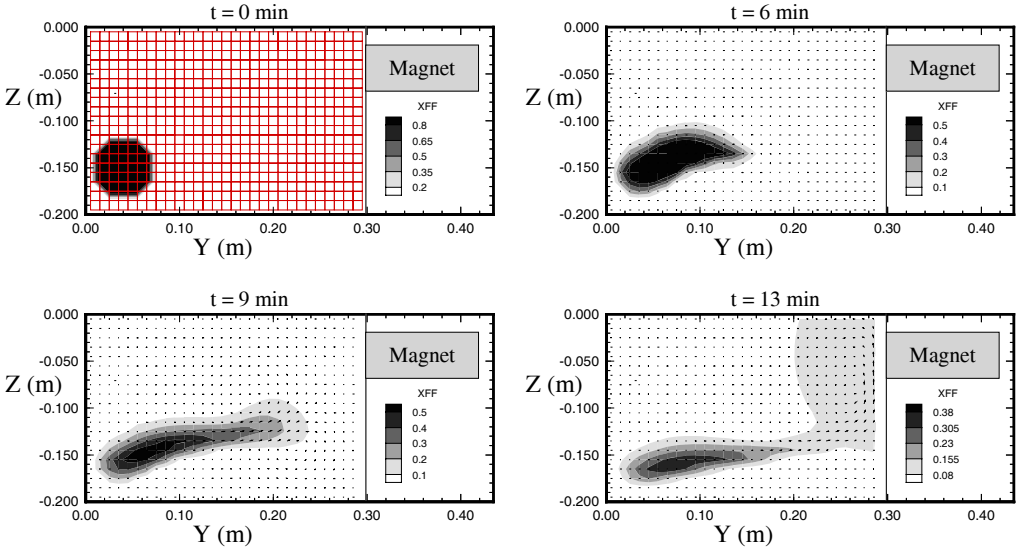

Fig. 7. Ferrofluid mass fraction and flow in Hele-Shaw cell simulation at t = 0 min, t = 6 min, t = 9 min, and t = 13 min.

Table 1. Properties of the Hele-Shaw cell flow simulation.

Domain	
Size (ΔY x ΔZ)	0.30 m x 0.20 m
Discretization for two-dimensional model	30 x 20 gridblocks of size 0.01 m square.
Permeability (k)	1.17×10^{-7} m^2
Porosity (ϕ)	0.999
Gravity (g)	0. m s^{-2}
Ferrofluid M-H curve fit:	
a1	1.00×10^{4} A m^{-1}
b1	3×10^{-5} m A^{-1}
	[i.e., M= 1.00×10^{4} A m^{-1} x arctan(3×10^{-5} m A^{-1} x H A m^{-1})]
Properties of the magnet (NdFeB)	
Residual flux density (B_r)	1.19 T
Size	5 x (2 in x 2 in x 1 in)
Properties of colloidal silica	
Viscosity of pure colloidal silica at T = 20 ˚C	4.5×10^{-3} kg m^{-1} s^{-1}
Density of pure colloidal silica at T = 20 ˚C	1200 kg m^{-3}
Properties of the ferrofluid (EMG 805)	
Viscosity of pure ferrofluid at T = 20 ˚C	2.35×10^{-3} kg m^{-1} s^{-1}
Density of pure ferrofluid at T = 20˚C	1190 kg m^{-3}

ferrofluid is taken as 2.35 x 10^{-3} Pa s. The plates are horizontal and gravity effects are ignored. After 6 minutes (upper right-hand frame), the ferrofluid has been slightly deformed in response to the magnetic field and its gradient. At t = 9 minutes, the fluid has moved strongly toward the magnet. Note that in this closed Hele-Shaw cell, there are recirculations caused by ferrfofluid motion. In other words, as ferrofluid is drawn from left to right in the system, pure water is displaced from right to left. Thus the flow of ferrofluid is affected by the water fluxes that occur in response to the ferrofluid flow. At t = 13 minutes, the ferrofluid has been attracted to the magnet and begun to cluster and circulate around the magnet. These results broadly matched the actual laboratory experiment in terms of flow geometry and time scales (Borglin et al., 1998). Differences arise primarily from numerical dispersion and associated mixing and dilution that occurs in the simulation and not in the laboratory Hele-Shaw cell.

CONCLUSIONS

We have developed EOS7M, a ferrofluid flow and transport module for TOUGH2. EOS7M calculates the magnetic forces on ferrofluid caused by an external magnetic field and allows simulation of flow and advective transport of ferrofluid-water mixtures through porous media. Such flow problems are strongly coupled and well suited to the TOUGH2 framework. Preliminary applications of EOS7M to some simple pressure and flow problems for which experiments were carried out in the lab show good qualitative agreement with the laboratory results.

ACKNOWLEDGMENT

We thank Yu-Shu Wu and Karsten Pruess for reviews. This work was supported by the Laboratory Directed Research and Development Program of Lawrence Berkeley National Laboratory under the U.S. Department of Energy, contract No. DE–AC03–76SF00098.

REFERENCES

Berkowsky, B.M., V.F Medvedev, M.S. Krakov, *Magnetic Fluids Engineering Applications*, Oxford Univ. Press, New York, 243 pp., 1993.

Borglin, S. E., and G.J. Moridis, Experimental studies of magnetically driven flow of ferrofluids through porous media, *Lawrence Berkeley Laboratory Report*, *LBL-40126*, March 1998).

Herbert, A.W., Jackson, C.P., and Lever, D.A., Coupled groundwater flow and solute transport with fluid density strongly dependent on concentration, *Water Res. Res.*, *24* (10), 1781-1795, 1988.

McCaig, Malcolm, *Permanent Magnets in Theory and Practice*, John Wiley & Sons, New York, 374 pp., 1977. pg. 187-188.

McCaig, Malcolm, and Alan G. Clegg, *Permanent Magnets in Theory and Practice Second Edition*, Halsted Press, John Wiley & Sons, New York, 415 pp., 1987. pg. 199-200.

Moridis, G.J., S.E. Borglin, C.M. Oldenburg, and A. Becker, Theoretical and experimental investigations of ferrofluids for guiding and detecting liquids in the subsurface, *Lawrence Berkeley Laboratory Report*, *LBL-41069*, March 1998).

Oldenburg, C.M., G.J. Moridis, and K. Pruess, EOS7M: Ferrofluid Flow for TOUGH2, in prep., 1998a.

Oldenburg, C.M., S.E. Borglin, and G.J. Moridis, Numerical simulation of ferrofluid flow for subsurface environmental engineering applications, in prep., 1998b.

Oldenburg, C.M. and K. Pruess, Dispersive transport dynamics in a strongly coupled groundwater-brine flow system, *Water Resources Research, 31*(2), 289–302, 1995.

Pruess, K., TOUGH User's Guide, *Nuclear Regulatory Commission, Report NUREG/CR-4645*, June 1987 (also *Lawrence Berkeley Laboratory Report*, *LBL-20700*, June 1987).

Pruess, K., TOUGH2- A general-purpose numerical simulator for multiphase fluid and heat flow, *Lawrence Berkeley Laboratory Report LBL-29400*, May 1991a.

Pruess, K., EOS7, An equation-of-state module for the TOUGH2 simulator for two-phase flow of saline water and air, *Lawrence Berkeley Laboratory Report LBL-31114*, Berkeley, California, August 1991b.

Raj, K., and R. Moskowitz, Commercial applications of ferrofluids, J. *of Magnetism and Magnetic Materials*, *85*, 233–245, 1990.

Reeves, M., Ward, D.S., Johns, N.D., and Cranwell, R.M., Theory and implementation of SWIFT II, the Sandia Waste-Isolation Flow and Transport Model for Fractured Media, *Report No. SAND83-1159*, Sandia National Laboratories, Albuquerque, N.M., 1986.

Rosenzweig, R.E., *Ferrohydrodynamics*, Cambridge University Press, 344 pp., 1985.